Contribution from the Institut für Physikalische und Theoretische Chemie, Freie Universität Berlin, Takustrasse 3, D-1000 Berlin 33, West Germany, Institut für Anorganische Chemie, J. W. Goethe-Universität Frankfurt, Niederurseler Hang, D-6000 Frankfurt/Main 50, West Germany, and Institut für Anorganische Chemie, Universität Dortmund, Otto-Hahn-Strasse, D-4600 Dortmund, West Germany

Photoelectron and Photoionization Mass Spectra of the Fluoramines $NH_{3-n}F_n$[1]

H. Baumgärtel,*[†] H.-W. Jochims,[†] E. Rühl,[†] H. Bock,*[‡] R. Dammel,[‡] J. Minkwitz,[§] and R. Nass[§]

Received November 19, 1987

The photoelectron and photoionization mass spectra of the recently prepared fluoramine (H_2NF) as well as of difluoramine (HNF_2), trifluoramine (NF_3), and ammonia have been recorded. The ionization patterns of the series $NH_{3-n}F_n$ are discussed by perturbation arguments based on semiempirical MNDO calculations, and their fragmentation pathways observed on photoionization are rationalized by comparison to both PE spectroscopic and theoretical results. From the molecular ionization energies and the fragment ion appearance potentials, thermochemical data such as heats of formation and bond dissociation energies have been calculated for the neutral molecules, their radical cations, and fragments.

Introduction

Both ammonia and nitrogen trifluoride, the molecules at both ends of the fluoramine series $NH_{3-n}F_n$ (n = 0–3) are thermally exceedingly stable. In contrast, difluoramine (HNF_2) is dangerous to handle even at low temperatures and often detonates in a seemingly spontaneous way.[2] This behavior can be rationalized by an exothermic decomposition into more stable products such as N_2 + HF.[3] Decomposition reactions in the case of NF_3 and NH_3 are endothermic. As concerns the missing fluoramine (H_2NF), its heat of formation probably exceeds that of HNF_2.[4] The thermal decomposition is expected to be exothermic as well. Therefore, it is not surprising that, after a long history of abortive attempts, pure H_2NF has only been prepared very recently[5] by decarboxylation of isopropyl fluorocarbamate in anhydrous HF, followed by low-temperature decomposition of the resulting fluoroammonium fluoride (cf. Experiment Section):

$$(CH_3)_2CH{-}O{-}\overset{\overset{O}{\|}}{C}{-}NHF \xrightarrow{HF} [H_3FN^+]HF_2^- \cdot nHF \xrightarrow[-HF]{240\ K} H_2NF \qquad (1)$$

fluoramine (H_2NF) is found to be stable only at low temperatures or at high dilution in the gaseous phase.[5] Its molecular structure has been characterized very recently by microwave spectroscopy.[6]

Photoionization methods such as photoelectron (PE) spectroscopy and photoionization mass (PIM) spectrometry are useful tools to study the electronic properties of molecules such as ionization potentials, fragmentation thresholds, and resonant processes.

Here we report both the photoelectron (PE) and photoionization mass (PIM) spectra for the series of fluoramines $NH_{3-n}F_n$, including ammonia. The assignment of their PE spectroscopic ionization patterns provides information not only on the various radical cation states but also for the interpretation of the PIM spectra. These in return yield appearance potentials, which allow one to calculate the binding energies of molecular cations and, by comparison with reference values, thermochemical data such as standard heats of formation for both neutral fluoramines and individual states of their radical cations.

Experimental Section

Preparation of H_2NF. The decarboxylation of isopropyl fluorocarbamate ($C_3H_7OC(O)NHF$) in anhydrous HF, which yields $[NH_3F^+]HF_2^-\cdot nHF$, has been described elsewhere.[5] Sublimation of this salt above 234 K leads to the production of HF and gaseous H_2NF. Advantageously and quantitatively, HF can be removed from the gas stream by passage through a 5-mm layer of activated KF under a dynamic vacuum.

The purity of H_2NF has been checked both by mass spectrometry (EI, 16 eV, m/z = 35 parent peak (100%)) and by IR spectroscopy (ν = 3346, 3234, 1564, 1241, 1233, and 891 cm^{-1}) in a 15 K N_2 matrix. At sublimation temperatures above 270 K, small amounts of NH_3 (968 cm^{-1}) and N_2H_2 (1340, 1285 cm^{-1}) are detected by matrix IR spectroscopy; presumably they are formed by HF elimination from H_2NF in the activated KF layer.

HNF_2 has been prepared according to the literature.[2] No significant impurities could be detected by mass spectrometry. Research grade ammonia has been supplied by Hoechst AG. No significant impurities, especially water, have been detected by PE spectroscopy.

Trifluoramine. NF_3 has been generously supplied by H. Bürger (Wuppertal, West Germany).

Photoelectron spectra have been recorded with a Leybold Heraeus UPG 200 spectrometer (cf. ref 7) with up to 50 000 counts/s and an average resolution of 20 meV. Calibration is based on the nitrogen ionizations $\tilde{X}(^2\Pi_u)$ = 15.60 eV and $\tilde{A}(^2\Sigma_g)$ = 16.98 eV.[8]

Photoionization mass spectroscopy experiments have been performed at the electron storage ring BESSY, Berlin, and involved a McPherson 225 1-m normal incidence monochromator, a quadrupole mass spectrometer, and a VUV photon detector described previously.[9]

Results and Discussion

Photoelectron Spectra and Their Assignments. Ionization Energies. According to a useful rule of thumb,[7] the number of ionizations in a He I measurement up to 21.21 eV should equal half the element p plus hydrogen 1s electrons. For the series $NH_{3-n}F_n$, therefore, $(3 + 3 - n + 5n)/2 = 2n + 3$ He I ionizations are expected, i.e. from three for NH_3[10] via five and seven for H_2NF and HNF_2[11] to nine for NF_3:[12] every substitution of H by F adds two ionizations from the formally nonbonding n_F lone pairs.

The PE spectra of ammonia and its fluoro derivatives (Figure 1) are advantageously[7] subdivided into two regions: the first one from 10 to 14 eV contains only fairly broad n_N lone-pair bands, all of which show extensive fine structure (Figure 2). The second region from 14 eV to the ionization limit of 21.21 eV exhibits $2n$

[†] Freie Universität Berlin.
[‡] J. W. Goethe-Universität Frankfurt.
[§] Universität Dortmund.

(1) Photoelectron Spectra and Molecular Properties. 112. Part 111: Dammel, R.; Bock, H. *J. Electron Spectrosc. Relat. Phenom.* **1986**, *41*, 311.
(2) Cf. e.g.: Lawton, E. A.; Weber, J. Q. *J. Am. Chem. Soc.* **1963**, *85*, 3595. Lawton, E. A.; Weber, J. Q. *J. Am. Chem. Soc.* **1959**, *81*, 4755.
(3) Pankratov, A. V.; Zercheninov, A. N.; Chesnokov, V. I.; Zhdanova, N. N. *Russ. J. Phys. Chem. (Engl. Transl.)* **1969**, *43*, 212.
(4) Smith, P.; Rao, C. N. R. *Can. J. Chem.* **1958**, *36*, 1174.
(5) Minkwitz, R.; Liedtke, A.; Nass, R. *J. Fluorine Chem.* **1987**, *35*, 307 and references therein. NHF_2 has also been prepared by the method in ref 2.
(6) Christen, D.; Minkwitz, R.; Nass, R. *J. Am. Chem. Soc.* **1987**, *109*, 7020.
(7) Bock, H.; Solouki, B. *Angew. Chem.* **1981**, *93*, 425; *Angew. Chem., Int. Ed. Engl.* **1981**, *20*, 427.
(8) Cf. e.g.: Bock, H.; Ramsey, B. G. *Angew. Chem.* **1973**, *85*, 773; *Angew. Chem., Int. Ed. Engl.* **1973**, *12*, 734.
(9) Rademann, K.; Jochims, H.-W.; Baumgärtel, H. *J. Phys. Chem.* **1985**, *89*, 3459.
(10) Cf. e.g.: Turner, D. W.; Baker, C.; Baker, A. D.; Brundle, C. R. *Molecular Properties Spectroscopy*; Wiley-Interscience: London, 1970. Kimura, K.; Achiba, Y.; Yamazaki, T.; Iwata, S. *Handbook of He(I) Photoelectron Spectra*; Halstead Press: New York, 1981.
(11) Colbourne, D.; Frost, D. C.; McDowell, C. A.; Westwood, N. P. C. *Chem. Phys. Lett.* **1980**, *72*, 247 and references therein. For SCF calculations of NHF_2 ionization potentials cf.: Minato, T.; Chong, D. P. *Chem. Phys. Lett.* **1980**, *72*, 252.
(12) Potts, A. W.; Lempka, H. J.; Streets, D. G.; Price, W. C. *Philos. Trans. R. Soc. London* **1970**, *A268*, 59. Basset, P. J.; LLoyd, D. R. *J. Chem. Soc., Dalton Trans.* **1972**, 248.

0020-1669/89/1328-0943$01.50/0

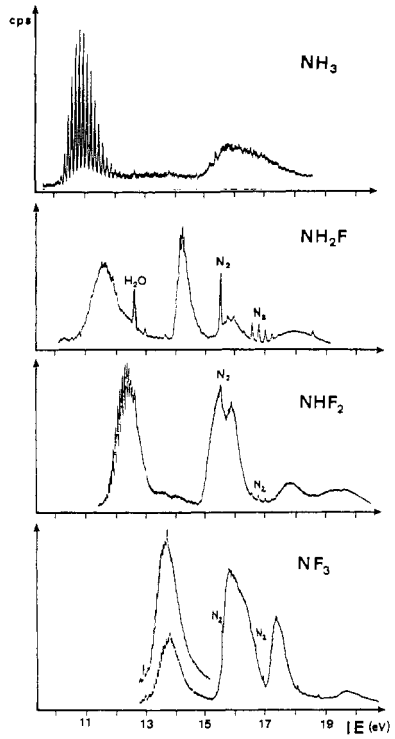

Figure 1. He I PE spectra of the fluoramines $NH_{3-n}F_n$ (calibrated by N_2; cf. Experimental Section).

Table I. Koopmans Correlation of Vertical Ionization Energies IE_n^v (eV) and MNDO Eigenvalues $-\epsilon_J^{MNDO}$ (eV) for Valence Electrons[a]

molecule	n/J	IE_n^v	Γ_J	$-\epsilon_J^{MNDO}$
NH_3	1	10.82	$2a_1$	11.2
	2	(15.8)	$1e^b$	16.7
	3	(16.5)		
H_2NF	1	11.62	5a′	11.7
	2	14.25	2a″	14.4
	3	15.9	4a′	16.7
	4	18.1	1a″	19.1
	5		3a′	19.3
NHF_2	1	12.38	6a′	12.6
	2	15.6	5a′	15.7
	3		4a″	16.1
	4	16.0	3a″	16.5
	5	18.0	4a′	18.4
	6	(19.3)	2a″	20.6
	7	(19.8)	3a′	20.9
NF_3	1	13.83	$4a_1$	13.9
	2	15.9	$1a_2$	16.8
	3	(16.3)	4e	17.0
	4	17.4	3e	17.4
	5	19.8	$3a_1$	20.0
	6	21.1[c]	2e	21.9

[a] Γ_J irreducible representations; see text. [b] Jahn/Teller-split radical-cation states. [c] Measured with He II.[12]

fluoro lone-pair ionizations n_F of the n fluorine substituents and two ionizations from the σ_{NH} or σ_{NF} bonds. As expected from the difference in effective nuclear charge between H and F, all ionization energies increase with F substitution (Figure 3 and Table I): the formation of the radical-cation ground states with predominant n_N contribution from 10.82 eV in NH_3 to 13.83 eV in NF_3, the center of the fluorine lone-pair ionizations $\overline{n_F}$ (Figure 3, O) from 15.1 eV in H_2NF to 17.2 eV in NF_3, and the center of the Jahn/Teller-split PE bands of NH_3 at 16.1 eV via 18.1 eV for H_2NF and 19.6 eV for HNF_2 to close to the 21.21-eV He I limit for NF_3.[12]

Radical-Cation-State Sequences. The well-established assignment of PE spectra via Koopmans correlation, $IE_n^v = -\epsilon_J^{SCF}$, with SCF eigenvalues often breaks down for small molecules containing several atoms of high effective nuclear charge such as F,[13] because

Chart I

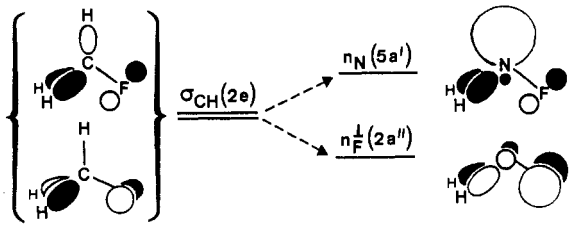

electron correlation and relaxation of the individual radical-cation state no longer approximately cancel.[13] To overcome these difficulties, the use of optimum parametrized semiempirical calculation procedures like MNDO[14] and, especially, a comparison with equivalent radical-cation states of chemically related, preferentially iso(valence)electronic molecules[15] are advisable. From the consistent PE spectroscopic discussion of other heavily fluoro-substituted nitrogen compounds,[16] MNDO eigenvalues (Table I) for the series $NH_{3-n}F_n$, yielding the regression

$$IE_n^v \text{ (eV)} = 0.578 + 0.937(-\epsilon_J^{MNDO}) \qquad (2)$$

with an acceptable correlation coefficient, $CORR^2 = 0.986$, as well as a radical-cation-state comparison with the iso(valence)-electronic fluoromethanes[17] $HCH_{3-n}F_n$ based on the "united atom" perturbation[18] HC ↔ N (Figure 3) will be chosen as independent approaches for the assignment.

We begin the generally accepted PE spectroscopic assignments and use the ionization patterns of NH_3 and CH_4[10] to illustrate the N ↔ CH perturbation approach. If one hydrogen of HCH_3 is formally shifted into the C nucleus, an N center with higher effective nuclear charge results, and accompanying the symmetry change $T_d \rightarrow C_{3v}$, the triply degenerate, Jahn/Teller-split $\sigma_{CH}(1t_2)$ radical-cation states transform into the nitrogen lone pair $n_N(2a_1)$ and into the $\sigma_{NH}(1e)$ states of $NH_3^{\bullet+}$ (Figure 3). For both CH_4 and NH_3, the center of these three valence ionizations remains constant as expected at ~14.3 eV (Figure 3).

In H_2NF the two n_F lone-pair ionizations at 14.2 and 15.9 eV (Figure 3, 2a″ and 4a′) are inserted between the former $n_N(2a_1)$ and $\sigma_{NH}(1e)$ PE bands of NH_3 (Figure 1). An analogous HC ↔ N perturbation argument for the iso(valence)electronic molecules HCH_2F and H_2NF together with the $C_{3v} \rightarrow C_s$ symmetry relation e → a′,a″ predicts both the $n_N(5a')$ and $n_F(2a'')$ states to originate from the $\sigma_{CH}(2e)$ state of $HCH_2F^{\bullet+}$ as can be visualized by qualitative molecular orbital diagrams (Chart I). For rationalization, removal of the proton potential from the eventual n_N lone-pair region leads to destabilization of the $n_N(5a')$ component. Simultaneous with the concurrent composition change (Chart I) the now $n_F^{\perp}$-dominated and bonding $n_F^{\perp}$ (2a″) orbital forms, additionally stabilized by the increase in effective nuclear charge HC → N. As can be gathered from Figure 3, the center of both the $\sigma_{CH}(2e)$ and of the $n_N(a') + n_F^{\perp}$ (2a″) ionizations remains approximately constant at around 14 eV. If the same reasoning is applied to the degenerate fluorine lone-pair state

(13) Cf. the review (quoting 406 references): Wittel, K.; Bock, H. Photoelectron Spectra of Organic Halogen Compounds. In *The Chemistry of Functional Groups*; Patai, S., Rappoport, Z., Eds.; Wiley: Chichester, England, 1983; p 1499–1603.
(14) Dewar, M. J. S.; Thiel, W. *J. Am. Chem. Soc.* **1977**, *98*, 4899. For the parametrization of the MNDO procedure cf.: Dewar, M. J. S.; Rzepa, H. S. *J. Am. Chem. Soc.* **1978**, *100*, 58.
(15) Bock, H. *Angew. Chem.* **1977**, *89*, 631; *Angew. Chem., Int. Ed. Engl.* **1977**, *16*, 613 and references therein.
(16) Examples are as follows. (a) $F_2HC—N_3$, $F_3C—N_3$, and $F_2C=NF$: Bock, H.; Dammel, R. *Angew. Chem.* **1987**, *99*, 503; *Angew. Chem., Int. Ed. Engl.* **1987**, *26*, 489; *Inorg. Chem.* **1985**, *24*, 4427. Bock, H.; Dammel, R.; DesMarteau, D. D. *Z. Naturforsch.* **1987**, *42B*, 308. (b) $F_3C—NC$ and $F_3C—CN$: Bock, H.; Dammel, R.; Lentz, D. *Inorg. Chem.* **1984**, *23*, 1535. (c) $(F_3C)_nN(CHF_2)_{3-n}$: Bürger, H.; Pawelke, G.; Dammel, R.; Bock, H. *J. Fluorine Chem.* **1982**, *19*, 565. See also literature citations and ref 13.
(17) Cf.: Bieri, G.; Asbrink, L.; von Niessen, W. *J. Electron Spectrosc. Relat. Phenom.* **1981**, *23*, 282 and references therein. See also ref 10.
(18) Cf. e.g. the PE spectroscopic comparison of H_2NCN and H_3CCN: Stafast, H.; Bock, H. *Chem. Ber.* **1974**, *107*, 1882.

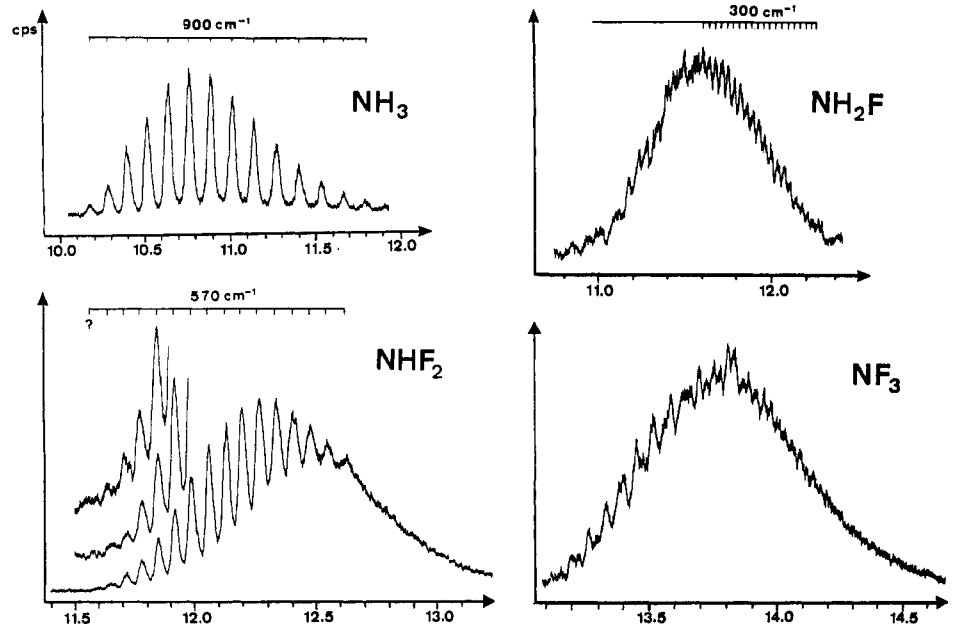

Figure 2. Extended-scale He I PE spectra of the first ionization bands of the fluoramines $NH_{3-n}F_n$.

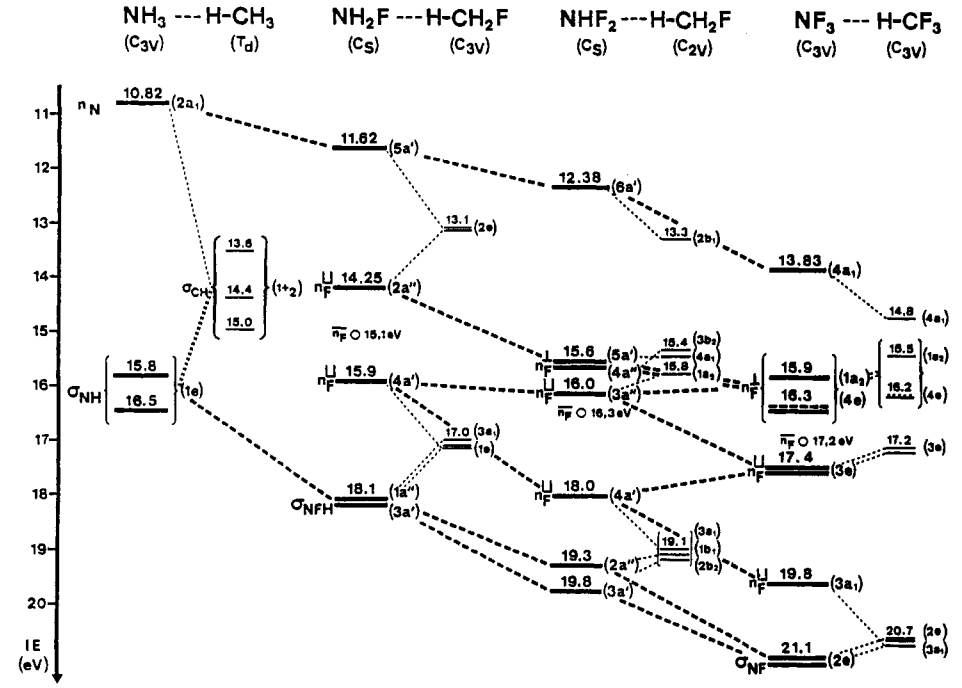

Figure 3. Radical-cation-state correlation diagram for the fluoramines $NH_{3-n}F_n$ (---) and iso(valence)electronic fluoromethanes $HCH_{3-n}F_n$[17] (···) ($\overline{n_F}$ = center of fluorine lone-pair ionizations; see text).

n_F(1e) of $HCH_2F^{\bullet+}$,[17] a split into another n_F(4a′) state and into the σ_{NFH}(1a″) state of $H_2NF^{\bullet+}$ follows. As denoted by $n_F^{\parallel}$ in Figure 3, the fluorine lone-pair lobes are parallel to the n_N lobe direction (cf. Chart I: n_N(5a′)). Again, the center of these ionizations at about 17 eV is approximately conserved (Figure 3). The accidental near-degeneracy of the $3a_1$ and the 1e states of $HCH_2F^{\bullet+}$ also reappears for the 1a″ and 3a′ states of $H_2NF^{\bullet+}$ (Figure 3). All the above HC ↔ N perturbation arguments are fully supported by the MNDO calculations (Table I).

For HNF_2 a total of four n_F ionizations are predicted and observed: according to PES band intensities, two at 15.6 eV and one each overlapping at about 16.0 eV and isolated at 18.0 eV (Figure 1).[11] According to the MNDO calculations (Table I), the corresponding radical-cation states are supposed to have the following dominating "+" hole contributions (Chart II, nodes visualized by orbital signs). Two of them exhibit fluorine lone-pair lobes perpendicular to the nitrogen lone-pair direction, $n_F^{\perp}$ (5a′) and $n_N^{\perp}$ (4a″), and two of them are either N/F antibonding

Chart II

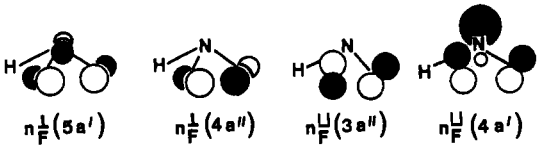

($n_F^{\perp}$(3a″)) or N/F bonding ($n_F^{\parallel}$(4a′)); the H atom, being situated in the C_s symmetry plane, does not contribute to any of these n_F-type radical-cation states (Chart II). Three of them are F/F antibonding, and one is F/F bonding (Chart II, 4a′), with the respective ionization energies being either smaller or larger than the averaged center $\overline{n_F}$ (Figure 3, ○). As concerns the correlation with the corresponding $HCHF_2^{\bullet+}$ states (Figure 3), the $C_{2v} \rightarrow C_s$ symmetry relations demand a_1, $b_1 \rightarrow a'$ and a_2, $b_2 \rightarrow a''$. Therefore, the n_F(4a″) and n_F(3a″) states of $HNF^{\bullet+}$, which correlate with the $n_F^{\perp}(3b_2)$ and $n_F^{\parallel}(1a_2)$ $HCHF_2^{\bullet+}$ states of

different symmetry, are also almost orthogonal to each other and interact only weakly (Figure 3). The effect of the HC ↔ N perturbation, i.e. removing the H potential from the area of the n_N lone-pair lobe, shows in the $n_F^{\parallel}(4a')$ states of both $H_2NF^{\bullet+}$ and $HNF_2^{\bullet+}$, which exhibit lower ionization energies than the comparable states of the fluoromethane radical cations,[17] i.e. 1e for $HCH_2F^{\bullet+}$ and $1b_1$ for $HCHF_2^{\bullet+}$ (Figure 3).

The NF_3 He I PE spectrum (Figure 1)[12] exhibits four bands, of which by intensity arguments the second one must contain three and the third one two ionizations. Because HCF_3 posesses the same C_{3v} skeleton symmetry, the Koopmans assignment based on MNDO eigenvalues (Table I) can be supported straightforwardly by comparison of the equivalent states of both iso(valence)electronic molecules, the only ambiguity being the sequence of the rather close $n_F^{\perp}(4e)$ and $n_F^{\perp}(1a_2)$ states.[17] Starting with the $n_N(4a_1)$ state, removal of the proton charge from the n_N region of high electron density leads—as for all other derivatives—to a lower ionization energy of NF_3. As concerns the slightly antibonding to nonbonding lone-pair states of $HCF_3^{\bullet+}$, $n_F^{\perp}(1a_2 + 4e)$ and $n_F^{\parallel}(3e)$, which due to symmetry contain no H contributions, they are expectedly stabilized in $NF_3^{\bullet+}$ due to the enhanced effective nuclear charge C → N. In contrast, the ionization energy into the bonding $n_F^{\parallel}(3a_1)$ state of $NF_3^{\bullet+}$ is lowered on n_N lone-pair formation HC → N as discussed already for the other iso(valence)electronic radical-cation pairs $HCH_2F^{\bullet+}/H_2NF^{\bullet+}$ and $HCHF_2^{\bullet+}/HNF_2^{\bullet+}$ (Figure 3).

In addition, the PES assignment for the series $NH_{3-n}F_n$ based on the well-parametrized[1] MNDO procedure (Table I) and on the $M^{\bullet+}$ state comparison with the iso(valence)electronic fluoromethanes $HCH_{3-n}F_n$ (Figure 3) can be further supported by numerous cross-linking correlations. Thus, the n_N ionization energies expectedly increase with the degree of F substitution (Figure 3): for NH_3 → H_2NF and for H_2NF → NHF_2 both increments $\Delta IE_1^v(n_N) \approx +0.8$ eV are observed; the considerably larger shift of +1.4 eV to 13.83 eV (!) for NF_3 (Figure 3) can be rationalized by the MNDO linear combination for its $n_N(4a_1)$ orbital, which is no longer antibonding but rather bonding. The center of the fluorine lone-pair ionizations (Figure 3: $\overline{n_F}$, ○) moves to higher energies in steps of 1.2 and 0.9 eV per additional F substituent. The fully geometry-optimized MNDO calculations, which reproduce reasonably well the known dipole moments of NH_3 (experimental 1.46 D, calculated 1.75 D) and NF_3 (experimental −0.24 D, calculated −0.20 D) predict the net atomic charges

	NH_3	H_2NF	NHF_2	NF_3
q_F		−0.16	−0.15	−0.14
q_N	−0.22	−0.02	+0.19	+0.42

The considerable net atomic N charge in NF_3 together with its trigonal-pyramidal structure (∠FNF = 106°) leads to the highest nitrogen lone-pair ionization energy known so far, even exceeding the value $IE_1^v(n_N) = 12.52$ eV for the nearly planar $N(CF_3)_3$.[16c] Relative to $N(CH_2SiR_3)_3$ with its rather low lone-pair ionization at only 7.66 eV,[19] altogether the span $\Delta IE_1^v(n_N) = 13.38 - 7.66 = 5.72$ eV results, indicating that the $NH_3^{\bullet+}$ radical-cation ground state is extremely substituent-sensitive and that fluorine ligands shift it most strongly to higher energy.

Vibrational Fine Structures. All four molecules $NH_{3-n}F_n$ investigated exhibit vibrational fine structures in their n_N ionization bands (Figures 1 and 2). In addition, the 14.22-eV ionization of H_2NF[10] also shows a vibrational progression (Figure 1).

The vibrational spacings observed for the individual radical cations $NH_{3-n}F_n$ differ considerably.

NH_3: The first band in its well-known PE spectrum[10] shows at least 18 resolved vibrational transitions with $\tilde{\nu}^+ = 900$ cm^{-1} (Figures 1 and 2).

H_2NF: The n_N lone-pair ionization band exhibits a complicated structure on its low-energy side and merges into a more regular progression with $\tilde{\nu}^+ = 300$ cm^{-1} at higher energies. In the second ionization band, five maxima with the spacing $\tilde{\nu}^+ = 550$ cm^{-1} are clearly distinguishable.

HNF_2: The structure in its first PE band,[11] although reminiscent of the NH_3 one (Figure 1), shows intervals of only $\tilde{\nu}^+ = 570$ cm^{-1}. Due to a rather weak 0 → 0 transition, the adiabatic ionization onset can be better estimated by the 11.5-eV appearance potential in the photoionization mass spectra (Figure 5 and next section).

NF_3: The vibrational progression $\tilde{\nu}^+ = 560$ cm^{-1} in its n_N ionization vanishes beyond the vertical ionization maximum.

To realize the different vibrational fine structures in the n_N ionization bands of the $NH_{3-n}F_n$ radical cations, the structural changes upon electron expulsion might offer some clues: whereas $NH_3^{\bullet+}$ becomes planar in its D_{3h} ground state,[21] $NF_3^{\bullet+}$ remains C_{3v} pyramidal.[20] The ground state of $HNF_2^{\bullet+}$ has been calculated to be planar,[11] and for $H_2NF^{\bullet+}$ MNDO calculations predict an also nearly planar structure. Pyramidal molecules posess a double-minimum potential in the inversion coordinate: with decreasing barrier height relative to the vibrational energy, the vibrational fine structure passes from clear separation at high barriers via a "chaotic" sequence of levels, if both are comparable, to "inversion doubling" at low barriers.[22] MNDO-approximated estimates of inversion barriers ΔE_{inv} (kcal/mol) for both neutral $NH_{3-n}F_n$ molecules and their radical cations paralleling ab initio values[23] for the neutral molecules M

	NH_3	H_2NF	NHF_2	NF_2
M	11	18	29	120
$M^{\bullet+}$	0	0	1	49

qualitatively reproduce the experimentally verified increase with F substitution.

The vibrational frequency $\tilde{\nu}^+ = 580 \pm 30$ cm^{-1} observed for the $HNF_2^{\bullet+}$ ground state has been extensively discussed and assigned to either reduced NH bending ($\tilde{\nu}_2 = 1307$ cm^{-1}) or increased NF_2 bending ($\tilde{\nu}_4 = 500$ cm^{-1}) relative to that in the neutral molecule.[11] As concerns the vibrational fine structure in the first PES band (Figure 2) of the hitherto unknown H_2NF, for which a force field analysis is not available, the following comments are proposed. The vibrational pattern of the n_N ionization band (Figure 2), exhibiting a complex structure on its low-energy side and a more regular progression with rather small spacings $\tilde{\nu}^+ = 300$ cm^{-1} beyond the vertical ionization maximum, would fit the expectation for a barrier penetration occurring around 11.6 eV. On the other hand, the MNDO estimates of ΔE_{inv} suggest a planar structure of $H_2NF^{\bullet+}$ and an almost negligible barrier for the next higher homologue $HNF_2^{\bullet+}$. Therefore, the rather small vibrational spacings observed for $H_2NF^{\bullet+}$ presumably cannot be explained by "inversion doubling", and an explanation of the complex dynamics of $H_2NF^{\bullet+}$ and $HNF_2^{\bullet+}$ possibly requires a model halfway between planar and trigonal pyramidal, analogous to the ones developed for "quasi-linear" molecules.[24]

Leading over to the following section, another fact of the vibrational fine structure in the n_N band of $HNF_2^{\bullet+}$ shall be pointed out: its disappearance above $\nu = 16$ at 12.63 eV (Figure 2) indicates a fragmentation process occurring above that threshold. According to exploratory MNDO calculations, an HF extrusion seems to be feasible:

$$HNF_2^{\bullet+} \rightarrow NF^{\bullet+} + HF \qquad \Delta H^{MNDO} \approx 0.25 \text{ eV} = 6 \text{ kcal/mol} \tag{3}$$

(19) Bock, H.; Kaim, W.; Kira, M. *J. Organomet. Chem.* **1979**, *164*, 295.

(20) Cf. e.g.: Potts, A. W.; Price, W. C. *Proc. R. Soc. London* **1972**, *A326*, 165. Aarons, L. J.; Guest, M. F.; Hall, M. B.; Hillier, I. H. *J. Chem. Soc., Faraday Trans. 2* **1973**, *69*, 643. See also ref 15.

(21) Cf. e.g.: Herzberg, G. *Molecular Spectra and Molecular Structure: Electronic Spectra of Polyatomic Molecules*; van Nostrand: New York, 1966. Berkowitz, J.; Greene, J. P. *J. Chem. Phys.* **1984**, *81*, 3383.

(22) Cf.: Ballard, R. E. *Photoelectron Spectroscopy and MO Theory*; Hilger: Bristol, England; p 69 ff. See also ref 20 and 21.

(23) Schmiedekamp, A.; Skaarup, S.; Pulay, P.; Boggs, J. E. *J. Chem. Phys.* **1977**, *66*, 5769 and references therein.

(24) For a review on quasi-linearity, cf.: Winnewisser, B. P. In *Molecular Spectroscopy and Modern Research*; Academic Press: New York, 1985; Volume 3, and references cited therein.

Table II. Relative Intensities of the Photofragments at 20.65-eV Photon Energy

molecule	cation	rel intens, %	molecule	cation	rel intens, %
NF_3	$NF_3^{\bullet+}$	67	H_2NF	$H_2NF^{\bullet+}$	51.5
	NF_2^+	16		NHF^+	1
	$NF^{\bullet+}$	17		$NF^{\bullet+}$	1.5
NHF_2	$NHF_2^{\bullet+}$	45		NH_2^+	44
	NF_2^+	0.5		$NH^{\bullet+}$	2
	NHF^+	43			
	$NF^{\bullet+}$	10.5			
	$NH^{\bullet+}$	1			

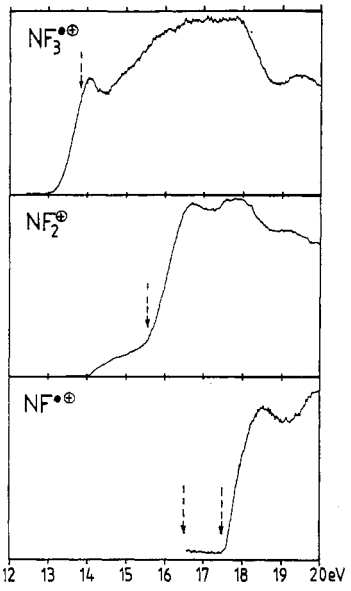

Figure 4. Photoionization efficiency of NF_3 as a function of photon energy (dashed arrows indicate vertical ionization potentials).

However, the threshold of ionic fragmentation observed in the photoionization mass spectra at 13.03 eV, 0.4 eV above the $\tilde{\nu}^+$ fine-structure limit, excludes any predissociation. To rationalize the experimental energy difference, the formation of the van der Waals nitrene complex $FH\cdots NF^{\bullet+}$ may be assumed, for which a binding energy of 9 kcal/mol is estimated and which would be analogous to carbene complexes like $H_2C\cdots HF^{\bullet+}$ formed on ionization of fluoromethane.[25]

Photoionization Mass Spectra. The photoionization efficiency (PIE) curves of the molecular ions as well as fragments arising from H_2NF, NHF_2, and NF_3 (Figures 4–6) and the relative abundances of the individual mass channels at 20.65 eV (Table II) will be discussed subsequently, beginning with NF_3.

NF_3. The appearance potentials measured are in good agreement with those from a previously published photoionization mass spectrum[26] and more recent coincidence work.[27] The sharp onset of the parent cation intensity corresponds to the formation of the NF_3^+ ground state ($\tilde{X}(^2A_1)$; cf. Figure 1). In the regime of 14 eV a broad autoionization structure is observed in the PIE curve of the parent ion. Here the fragmentation into $NF_2^+ + F$ starts, which may be a result of a dissociative autoionization process. A second onset at 15.5 eV may be due to electronic predissociation of the second NF_3^+ state (Figure 3, $1a_2$). Above 17.5 eV NF^+ is formed. The steep onset suggests direct dissociation or predissociation of the third NF_3^+ state (cf. Figure 3, 4e). This would favor a simultaneous fragmentation into $NF^+ + F_2$. However, Mansell et al.[27] and Baer et al.[28] have also invoked a sequential mechanism according to the equation

$$NF_3^+ \rightarrow NF_2^+ + F \rightarrow NF^+ + F + F \qquad (4)$$

Unfortunately with both the state-selected coincidence experiment[27] and a statistical model[28] none of the mechanisms could be favored unambiguously but thermochemical arguments support the sequential formation of NF^+ as discussed in the next section.

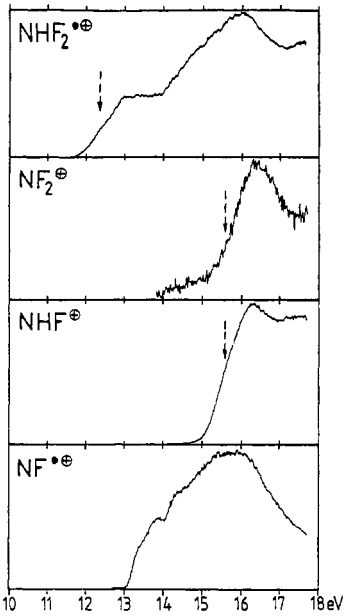

Figure 5. Photoionization efficiency of NHF_2 as a function of photon energy (dashed arrows indicate vertical ionization potentials).

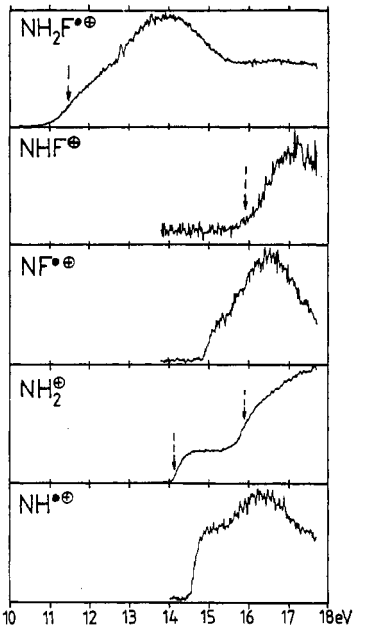

Figure 6. Photoionization efficiency of H_2NF as a function of photon energy (dashed arrows indicate vertical ionization potentials).

(25) Halim, H.; Ciommer, B.; Schwarz, H. *Angew. Chem.* **1982**, *94*, 547; *Angew. Chem., Int. Ed. Engl.* **1982**, *21*, 528. Cf. also the reviews by: Schwarz, H. *Nachr. Chem., Tech. Lab.* **1983**, *31*, 451. Radom, L.; Bonna, W. J.; Nobes, R. H.; Yates, B. F. *Pure Appl. Chem.* **1984**, *56*, 1831.
(26) Dibeler, V. H.; Walker, J. A. *Inorg. Chem.* **1969**, *8*, 1728.
(27) Mansell, P. I.; Danby, C. J.; Powis, I. *J. Chem. Soc., Faraday Trans. 2* **1981**, *77*, 1449.
(28) Baer, T.; DePristo, A. E.; Hermans, J. J. *J. Chem. Phys.* **1982**, *76*, 5917.
(29) Robin, M. B. *Higher Excited States in Polyatomic Molecules*; Academic Press: New York, 1974; Vol. 1.
(30) Chase, M. W.; Cornutt, J. L.; Downey, J. R.; McDonald, R. A.; Syvernd, A. N.; Valenzuela, E. A. JANAF Tables (1982 Supplement). *J. Phys. Chem. Ref. Data Ser.* **1982**, *11*, 695.
(31) Stull, D. R.; Prophet, H. *JANAF Thermochemical Tables*, 2nd ed.; NSRDS-NBS: Washington, DC, 1971.
(32) Wagman, D. D.; Evans, W. H.; Parker, V. B.; Schumm, R. H.; Halow, I.; Bailey, S. M.; Churney, K. L.; Nuttall, R. L. *J. Phys. Chem. Ref. Data Ser.* **1982**, *11* (Suppl. 2).
(33) Sloan, J. J.; Waston, D. G.; Wright, J. S. *Chem. Phys.* **1981**, *63*, 283.

Table III. Reference Heats of Formation ΔH_f (kcal/mol) Used for Thermochemical Calculations within the $NH_{3-n}F_n$ Series

species	ΔH_f	ref	species	ΔH_f	ref
NH_3	−10.97 ± 0.1	30	HF	−65.14 ± 0.2	30
H_2NF	−5[a]	4	$NH_2^\bullet$	45.5 ± 1.5	30
NHF_2	−15.6 ± 1.5	3	NH	84.0	32
NF_3	−31.57 ± 0.27	30	$NHF^\bullet$	25.5 ± 4[a]	33
$H^\bullet$	52.103 ± 0.001	30	$NF_2^\bullet$	10.1 ± 2	31
$F^\bullet$	18.86 ± 0.4	31	NF	59.5 ± 8	31

[a] Estimated value.

NHF_2. The $NHF_2^{\bullet+}$ parent ion curve (Figure 5) differs considerably from that of $NF_3^{\bullet+}$ (Figure 4). Two increase steps are observed, one corresponding to the $NHF_2^{\bullet+}$ ground state ($\tilde{X}(^2A')$; cf. Figure 1), and a second one at 14.0 eV, which cannot be attributed to the predissociation of a stable ionic state because of the energy gap observed in the PE spectrum (cf. Figure 1). Therefore, this feature might be mainly due to autoionization of a yet unknown "superexcited state" in the neutral NHF_2 molecules which is followed by vibrational predissociation into NF^+ mainly. According to term value considerations,[26] a $3a'' \rightarrow 3p$ Rydberg transition might be expected at about 14 eV. These excitations give rise to so called D bands in the VUV spectroscopy of halocarbons and show significant intensities.[26] Another interesting feature of the NHF_2 photoionization efficiency curves (Figure 5) is the rather steeply rising segment of the $NF^{\bullet+}$ fragment ion curve, which again cannot be assigned to a corresponding PES band, because the NHF_2 PE spectrum (Figure 1) between 13 and 15 eV shows only a low-intensity noise level background. The measurements performed, however, yield no information as to what extent direct dissociation and/or autoionization of "superexcited" states are involved in the formation of the $NF^{\bullet+}$ radical cations.

H_2NF. According to the photoionization efficiency curves (Figure 6), its most intensive fragmentation yields NH_2^+ ions. The photoion curve of NH_2^+ shows two distinct onsets. The lower one starts at 14.1 eV and is interrupted by the onset of the $NH^{\bullet+}$ fragmentation at 14.6 eV as a competitive reaction resulting from predissociation of the second ionic state. The second onset at 15.6 eV originally results from direct dissociation of the third $H_2NF^{\bullet+}$ state ($\tilde{B}(^2A')$; cf. Figure 3), which results from fluorine lone-pair ionization.

Thermochemical Considerations. From the observed fragmentation reactions, thermodynamic properties such as heats of formation and bond dissociation energies can be derived on the basis of the energy relation

$$AP = IP + D = \Delta H_f(\text{products}) - \Delta H_f(\text{neutral molecules}) \quad (5)$$

AP denotes the appearance potential of the ionic fragment, IP is the adiabatic ionization potential of the molecule into its radical cation ground state, D is the dissociation energy into the respective molecular ion, and ΔH_f values are standard heats of formation. Excess energies that influence the measured AP's are not considered in (5). For the subsequent thermochemical considerations, the reference data (Table III) have been used.

NF_3. Its parent ions are generated at 13.06 eV, corresponding to the heat of formation $\Delta H_f(NF_3^{\bullet+}) = 269.8$ kcal/mol. At the lowest fragmentation energy of 14.10 eV, NF_2^+ ions are produced according to

$$NF_3 + h\nu \rightarrow NF_2^+ + F^\bullet + e^- \quad (6)$$

From the reference data (Table III) $\Delta H_f(NF_2^+) = 274.7$ kcal/mol is evaluated. Starting in an independent approach from the adiabatic ionization potential determined PE spectroscopically for the $NF_2^\bullet$ radical, $IP(NF_2^\bullet) = 11.62$ eV,[34] and adding $\Delta H_f(NF_2^\bullet) = 10.1$ kcal/mol (Table III) yields $\Delta H_f(NF_2^+) = 278$ kcal/mol for the direct ionization process. Judging from reasonable agreement of both values and that reported in the literature, $\Delta H_f(NF_2^+) = 279.7$ kcal/mol,[32] obviously, no excess energy is released in the fragmentation process (6). This agrees with the kinetic energy release measurements in ref 27, where a slow statistical dissociation process is deduced. This has been confirmed by phase-space model calculations.[27]

The appearance of $NF^{\bullet+}$ ions is observed at 17.50 eV. For the respective reaction

$$NF_3 + h\nu \rightarrow NF^{\bullet+} + 2F^\bullet + e^- \quad (7)$$

one calculates, using the reference data in Table III, $\Delta H_f(NF^{\bullet+}) = 334 \pm 2$ kcal/mol. Unfortunately, one cannot distinguish between primary and secondary dissociation using only thermochemical arguments.[27] However, it seems to be quite reasonable that the formation of F_2 instead of 2 $F^\bullet$ is favored by thermochemical arguments. Therefore, a sequential process leading to NF^+ seems to be more adequate to describe this reaction.

Subtracting the PE spectroscopic ionization potential for neutral NF, IP(NF) = 12.26 eV,[35] yields $\Delta H_f(NF) = 51 \pm 2$ kcal/mol, which might be more reliable than the tabulated reference value (cf. Table III: $\Delta H_f(NF) = 59.9 \pm 8$ kcal/mol). For reaction 7, therefore, no fragmentation excess energy has to be taken into account.

NHF_2. Its heat of formation has been determined calorimetrically to amount to $\Delta H_f(NHF_2) = -15.6 \pm 1.5$ kcal/mol.[3] For the $NHF_2^{\bullet+}$ ion, the adiabatic ionization potential, $IP(NHF_2) = 11.60$ eV (Figure 2), together with the NHF_2 reference value (Table III) yields $\Delta H_f(NHF_2^{\bullet+}) = 252 \pm 2$ kcal/mol. Fragmentation to $NF^{\bullet+}$ ions

$$NHF_2 + h\nu \rightarrow NF^{\bullet+} + HF + e^- \quad (8)$$

starts at 13.03 eV (Figure 5). When $\Delta H_f(NF^{\bullet+}) = 334$ kcal/mol from reaction 7 is combined with $\Delta H_f(HF)$ and $\Delta H_f(NHF_2)$ from Table IV, a thermodynamic threshold of 12.34 eV is expected. The difference $\Delta AP = 13.03 - 12.34 = 0.7$ eV represents the excess energy in reaction 8 and has to be either transferred into kinetic energy of the fragments or stored as internal energy. On photoionization above 14.2 eV, fluoramine cations NHF^+ are detected:

$$NHF_2 + h\nu \rightarrow NHF^+ + F^\bullet + e^- \quad (9)$$

The calculated $\Delta H_f(NHF^+) = 293$ kcal/mol together with the estimate $\Delta H_f(NHF^{\bullet+}) = 25.5$ kcal/mol[33] from semiempirical calculations allows us to predict the adiabatic ionization potential $IP(NHF^{\bullet+}) = 11.6$ eV. Above 15.1 eV the formation of NF_2^+ fragments is observed:

$$NHF_2 + h\nu \rightarrow NF_2^+ + H^\bullet + e^- \quad (10)$$

Although the intensity is rather weak (Table II), the derived heat of formation $\Delta H_f(NF_2^+) = 280 \pm 5$ kcal/mol is in agreement with the more precise value $\Delta H_f(NF_2^+) = 278 \pm 1$ kcal/mol from the direct ionization process (cf. discussion of reaction 6) and, therefore, excess energy contributions can probably be neglected.

H_2NF. For this molecule, no experimentally determined gas-phase heats of formation have been reported so far; the only literature value,[4] $\Delta H_f(H_2NF) = -5$ kcal/mol (Table III), represents an estimate. Photofragmentation supports this value by comparing both the dominant H_2NF reaction (Table III) occurring above 14.10 eV

$$H_2NF + h\nu \rightarrow NH_2^+ + F^\bullet + e^- \quad (11)$$

and the precisely studied NH_3^+ fragmentation[36]

$$NH_3 + h\nu \rightarrow NH_2^+ + H^\bullet + e^- \quad (12)$$

With $\Delta H_f(NH_2^+) = 300.5$ kcal/mol derived from $AP(NH_2^+) = 15.768$ eV[36] and $\Delta H_f(NH_3) = -10.97$ kcal/mol (Table III), the value $\Delta H_f(H_2NF) = -6 \pm 1$ kcal/mol is indirectly calculated for reaction 11. Both the proven absence of kinetic excess energy in reaction 12[37] and the surprisingly good agreement of the estimated (Table III) and the indirectly calculated H_2NF heats of formation

(34) Cornford, A. B.; Frost, D. C.; Herring, F. G.; McDowell, C. A. *J. Chem. Phys.* **1971**, *54*, 1872.
(35) Dyke, J. M.; Jonathan, N.; Lewis, A. E.; Morris, A. *J. Chem. Soc., Faraday Trans. 2* **1982**, *78*, 1445.
(36) McCulloh, K. E. *Int. J. Mass Spectrom. Ion Phys.* **1976**, *21*, 333.
(37) Powis, I. *J. Chem. Soc., Faraday Trans. 2* **1981**, *77*, 1433.

Table IV. Heats of Formation ΔH_f (kcal/mol) of $NH_xF_n^+$ Ions

species	ΔH_f this work	ΔH_f lit.	species	ΔH_f this work	ΔH_f lit.
$NF_3^{\bullet+}$	269.8	271[a]	NHF^+	293 ± 4	
$NHF_2^{\bullet+}$	252 ± 2		NH_2^+	300.5	303.5[b]
$H_2NF^{\bullet+}$	244 ± 2		$NF^{\bullet+}$	334 ± 2	339[c]
$NH_3^{\bullet+}$	223.6	225[a]	$NH^{\bullet+}$	394 ± 1	396.3[d]
NF_2^+	278 ± 1	279.7[b]			

[a] Reference 39. [b] Reference 32. [c] Reference 39. [d] Reference 38.

Table V. N–F and N–H Bond Dissociation Energies D (kcal/mol) for Neutral Molecules $NH_{3-n}F_n$ and Their Cations $NH_{3-n}F_n^+$

bond	$D(NH_{3-n}F_n)$	$D(NH_{3-n}F_n^+)$
F_2N–F	61	27
FHN–F	60	60
H_2N–F	69	75
F_2N–H	78	78
FHN–H	83	101
H_2N–H	109	129

justify the application of this value in the subsequent discussions of fragmentation channels. For $H_2NF^{\bullet+}$, the heat of formation $\Delta H_f(H_2NF^{\bullet+}) = 244 \pm 2$ kcal/mol is evaluated from the adiabatic ionization potential $IP(H_2NF) = 10.83$ kcal/mol (Figures 2 and 6). $NF^{\bullet+}$ fragment ions are formed above 14.85 eV (Figure 6):

$$H_2NF + h\nu \rightarrow NF^{\bullet+} + H_2 + e^- \quad (13)$$

The value $\Delta H_f(NF^{\bullet+}) = 334$ kcal/mol obtained from this reaction is in excellent agreement with that from reaction 7. In addition, imino cations NH^+ are produced at 14.50 eV according to

$$H_2NF + h\nu \rightarrow NH^{\bullet+} + HF + e^- \quad (14)$$

Again, the value $\Delta H_f(NH^{\bullet+}) = 394$ kcal/mol calculated by using the reference data (Table III) agrees perfectly with $\Delta H_f(NH^{\bullet+}) = 396.3$ kcal/mol, recently measured by photoionization mass spectrometry of $NH_2^{\bullet}$ radicals.[38] In conclusion, the rather weak $NHF^{\bullet+}$ fragment ion intensity (Table II) in the photoionization efficiency curves of H_2NF (Figure 6) shows an onset at 15.2 eV:

$$H_2NF + h\nu \rightarrow NHF^+ + H + e^- \quad (15)$$

The heat of formation $\Delta H_f(NHF^+) = 292 \pm 3$ kcal/mol from reaction 15 confirms the value of 293 kcal/mol from the respective NHF_2 fragmentation (9).

The heats of formation for the ions $NH_{3-n}F_n^+$, $NH_{2-n}F_n^+$, and $NH_{1-n}F_n^+$ evaluated from the photoionization mass spectroscopy data (Figures 4–6) are summarized in Table IV). Comparison with available literature data (Table IV) demonstrates the rather satisfying agreement.

Bond Dissociation Energies. From the heats of formation for the neutral molecules $NH_{3-n}F_n$ (Table III) and their respective cations $NH_{3-n}F_n^+$ (Table IV) fluorine and hydrogen abstraction energies can be derived (Table V). The approximated dissociation energies for N–H bonds expectedly exceed those for N–F bonds due to the higher energy content of the H$^{\bullet}$ atoms (Table III) produced. The increase with decreasing F substitution can be correlated with the increasing destabilization of the radicals formed, $NF_2^{\bullet} > NHF^{\bullet} > NH_2^{\bullet}$, and the increasing stabilization of the parent compounds, $NF_3 > NHF_2 > H_2NF$ (Table III). The N–H bond breaking difference between neutral molecules and their cations is largest for H_2NF (Table V) and results from opposing sequences of the radical cations $NH_{3-n}F_n^{\bullet+}$ and the cations $NH_{2-n}F_n^+$ (Table IV). As concerns the N–F bonds, which exhibit nearly constant dissociation energies for the neutral fluoroamines $F_nH_{2-n}NF$, a dramatic decrease is observed on ionization $NF_3 \rightarrow NF_3^{\bullet+}$, causing a drop to less than half the value for neutral NF_3 (Table V). In tracing this effect, one detects the unusually small difference of only 8 kcal/mol in the heats of formation of $NF_3^{\bullet+}$ and NF_2^+ being mainly due to the exceptionally high first ionization potential of NF_3 (Figure 3). Relative to the planar ground state of $NH_3^{\bullet+}$, the still pyramidal $NF_3^{\bullet+}$ ion requires ~3 eV = 70 kcal/mol for its vertical generation. As discussed in the PE spectroscopic section, antibonding n_F interactions with n_N lone pairs in H_2NF and NHF_2 on n_N ionization lead to higher N–H and N–F binding components in the radical cations generated (Tables I, III, and IV). The n_N lone pair in NF_3, however, is bonding, and removal of one of its electrons to form $NF_3^{\bullet+}$ reduces the N–F binding energy contribution considerably (Table V).

Concluding Remarks

The combination of PE spectroscopy and PIM spectrometry supported by quantum-chemical model calculations and applied to the series of fluoramines $NH_{3-n}F_n$, including ammonia, reveals an intriguing picture of their photoionization followed by fragmentation of the cations generated. The properties of the individual radical-cation states as discussed in the PE spectroscopic section influence the fragmentation behavior of the molecular cations as observed by PIM spectrometry. Some of the fragmentation appearance potentials correlate with adiabatic ionization potential.

Acknowledgment. The investigations, to which three independent groups have contributed, were generously supported by the Deutsche Forschungsgemeinschaft, the Fonds der Chemischen Industrie, and the Bundesministerium für Forschung und Technologie (H.B., H.-W.J., E.R.).

Registry No. H_2NF, 15861-05-9; HNF_2, 10405-27-3; NF_3, 7783-54-2; NH_3, 7664-41-7; NF_3^+, 54384-83-7; HNF_2^+, 118476-90-7; H_2NF^+, 110618-91-2; NH_3^+, 19496-55-0; NF_2^+, 31685-31-1; NHF^+, 42080-79-5; NH_2^+, 15194-15-7; NF^+, 3146-37-0; NH^+, 19067-62-0.

(38) Gibson, G. T.; Greene, J. P.; Berkowitz, J. *J. Chem. Phys.* **1985**, *83*, 4319.
(39) Rosenstock, H. M.; Draxl, K.; Steiner, B. W.; Herron, J. T. *J. Phys. Chem. Ref. Data Ser.* **1977**, *6* (Suppl. 1).